ELSEVIER

S0032-3861(96)00172-3

Polymer Vol. 37 No. 16, pp. 3509–3519, 1996
Published by Elsevier Science Ltd
Printed in Great Britain
0032-3861/96/$15.00+0.00

Morphology control and interfacial reinforcement in reactive polystyrene/amorphous polyamide blends

N. C. Beck Tan*, S.-K. Tai and R. M. Briber†
Department of Materials and Nuclear Engineering, University of Maryland, College Park, MD 20742, USA
(Received 4 October 1995; revised 22 November 1995)

The effects of reactive compatibilization on blend morphology and interfacial adhesion in the polystyrene (PS)/amorphous polyamide (aPA) system were investigated. Reactivity was incorporated onto the polystyrene component by copolymerization with ~1% of vinyl oxazoline which is reactive with the amorphous polyamide end-groups. The reaction between oxazoline and polyamide end-groups produces interchain bonds and the *in situ* generation of copolymers. Incorporation of reactivity into this system has resulted in significant refinement of the blend morphology, with the dispersed phase size in the reactive blend reduced by ~60% relative to the unreactive blend. The grafting reaction was verified and quantified using infra-red spectroscopy, which indicated that ~2.5 wt% of PS-*g*-aPA compatibilizer was formed during blend processing. In addition to stabilizing the microstructure, *in situ* compatibilization was found to alter the mechanical properties of the PS/aPA interface. Evaluation of adhesion at both the reactive interface and its unreactive counterpart revealed that the reactive interface was mechanically reinforced by copolymer formation, and typically showed fracture toughness at least twice that of the unreactive interface. Published by Elsevier Science Ltd.

(Keywords: blends; morphology; interfacial adhesion)

INTRODUCTION

There has been significant commercial interest over the last two decades in producing improved materials through blending of commercially available polymers rather than through synthesis of new polymers[1,2]. However, difficulties arise in the blending of polymers owing to the inherent thermodynamic incompatibility in mixtures of long-chain molecules[1–3]. This incompatibility often results in blends having a microscopically heterogeneous structure in which the interfaces are compositionally sharp and mechanically weak. Because the properties of immiscible blends are strongly dependent on the size and distribution of the phases (i.e. the blend morphology) and on the adhesion at the interfaces, development efforts are concerned with control of these aspects of blend structure.

Traditionally, morphology control has been achieved through compatibilization techniques in which block copolymers are incorporated into the blend. While the utility of block copolymers for controlling the morphology of immiscible blends has been established for a variety of systems[1–4], the effects of block copolymer addition on interfacial adhesion have been more difficult to assess. Recently, effort has been concentrated specifically on evaluating adhesion at block copolymer compatibilized interfaces by isolating the interface and measuring its mechanical properties using a model sample geometry. These efforts have shown that interphase adhesion may be dramatically improved by addition of copolymer at the interface, provided the reinforcing copolymers are present in high enough concentration and the copolymer blocks are of sufficient molecular weight[5–12]. Unfortunately, the conditions favouring good interfacial adhesion are often difficult to achieve in commercially processed blends where the amount of added copolymer which may be dispersed to the interfaces is limited by mixing efficiency and the formation of copolymer micelles. Due to these difficulties, efforts have been redirected towards *in situ* compatibilization methods, in which copolymers are formed at the interfaces during processing through the interaction of functional groups incorporated onto the blend components. This 'reactive compatibilization' may be accomplished through various types of functional group interaction and potentially offers a simple and cost-efficient route to morphological control in immiscible blends[13–15]. Reactive compatibilization methods have been demonstrated to be effective in controlling morphology in a variety of systems, with the degree of morphology refinement achieved dependent on the amount of reactivity introduced[16–19] and the type of co-reactive pair employed[20].

Though modifications to blend morphology through reactivity have been well documented, the effects of

* Present address: Army Research Laboratory, Attn: AMSRL-MA-PB, CNR Site, APG, MD 21005-5069, USA
† To whom correspondence should be addressed

in situ copolymer formation on the interphase adhesion in immiscible reactive blends has received little attention. Liu and Baker[21–23] have used a novel approach to estimate the interfacial adhesive effects of reactivity indirectly from blend mechanical properties by attempting to eliminate the morphology as a variable through rigorous control of processing conditions of unreactive blends. Their investigations showed that the impact strengths of reactively modified, rubber/thermoplastic blends were superior to those of the unreactive counterparts at essentially constant morphology, implying that improved interfacial adhesion was responsible for the superior mechanical properties. Direct evaluation of interfacial properties in a reactive system has been documented only recently. In one study[24], the addition of a thin layer of a reactive polystyrene (PS)–17% styrene maleic anhydride copolymer to the interface between PS and an amorphous polyamide (aPA) was shown to result in greatly enhanced adhesion. In a second investigation, significant improvements in interfacial adhesion were achieved at polystyrene/poly(2-vinyl pyridine) interfaces once the styrene was functionalized by sulfonation, creating sites which interact ionically with the pyridine nitrogen[25]. The latter study has indicated that improvements in interfacial properties are most significant in systems of relatively high reactivity. In blended materials, high reactivities generally also lead to large reductions in dispersed phase size; however, in many cases the goal of compatibilization is to control the particle size, rather than to achieve a maximum particle size reduction. Therefore, the conditions corresponding to successful interfacial strengthening may result in a blend morphology which is refined beyond the useful range.

It is the aim of this investigation to address the issue of morphology refinement in a blend of modest reactivity, and to assess the effects of reactivity on the interfacial properties under these conditions. A polystyrene/amorphous polyamide (PS/aPA) blend system was chosen for study. A commercial reactive polystyrene which has been functionalized by copolymerization of styrene with vinyl oxazoline is used. The oxazoline group is reported to be highly reactive, capable of forming covalent bonds with a variety of moieties, such as amine, carboxyl, epoxy, hydroxyl and anhydride groups[13]. The reaction of interest in the poly(styrene-*co*-oxazoline) (PS-ox)/aPA system is between the oxazoline ring and the carboxyl and amine end-groups common to polyamides produced by condensation polymerization. Previous investigations in PS/polyethylene[26–28], acrylonitrile–butadiene/PS[29] and acrylonitrile–butadiene/polypropylene[21] have demonstrated the effectiveness of the co-reactive pair carboxylic acid/oxazoline for forming interchain grafts during blend processing, even at very low oxazoline content (<1%). The oxazoline-modified polystyrene (PS-ox)/aPA system was chosen for its practical significance, and also to evaluate the efficiency of the oxazoline functionality as a compatibilizing agent for polyamide blends.

The results of the present investigation clearly demonstrate that the addition of oxazoline functional groups to polystyrene produces refinement of PS/aPA blend morphology. A post-processing, quantitative evaluation was made of the blend confirming the formation of ~2.5 wt% of compatibilizer. In addition, interfacial fracture studies have shown that the *in situ* generation of PS-*g*-aPA copolymers due to the reaction provides modest mechanical reinforcement, with adhesion at the reactive interface being approximately twice that of the unreinforced one.

EXPERIMENTAL

Materials

The reactive polystyrene used in this investigation is a product of copolymerization of styrene and vinyl oxazoline and was purchased from Scientific Polymer Products. The vinyl oxazoline content was determined to be 1.18 mol% by Galbraith Laboratories. Two commercial polystyrenes were used in the control studies. The first, Dow Styron 666, was used in blending studies. The second, obtained from Aldrich Chemical, was used in interfacial adhesion studies. Molecular weights of all polystyrenes were obtained by g.p.c. using polystyrene standards and are reported in *Table 1*. The amorphous polyamide (aPA) used in this study was Grilamid TR55, obtained from EMS-American Grilon. It is a random copolymer of isophthalic acid, 12-aminododecanoic acid, and bis(4-amino-3-methylcyclohexyl) methane, which are present in the molar ratio 1.0 : 1.057 : 1.0 (ref. 30). This material is believed to be synthesized through a condensation process resulting in amine and carboxylic acid end-groups.

Blends

PS/aPA and PS-ox/aPA blends were prepared in composition ratios of 1 : 99 and 20 : 80 by weight. The reactions responsible for compatibilization in the PS-ox/aPA system are illustrated schematically in *Figure 1*. Oxazoline groups (grafting sites) are believed to be approximately randomly distributed along the PS-ox chains.

Blends were prepared by melt-mixing in a Banbury mixer driven by a Brabender Plasticorder. The mixer was operated at 70% fill level to optimize break-up and mixing uniformity[31]. Due to moisture sensitivity, aPA pellets were dried in vacuum at 80°C for a minimum of 16 h immediately prior to processing. PS or PS-ox and aPA pellets were then dry-blended, added to the equipment which had been preheated to 180°C, and mixed at 50 rev min^{-1} for 10 min. Mixer temperature typically reached 205–210°C during blending owing to viscous heat generation. After mixing, the blend was quenched in cold water to minimize post-processing development of the microstructure.

Table 1 Rheological properties

Material	M_w^a (g mol^{-1})	M_n^a (g mol^{-1})	Melt index (g min^{-1})	Processing temperature (°C)	Torque ratio PS/aPA
PS-ox	230 000	90 200	7[c]	200–208	0.168
PS (Aldrich)	315 000	97 000	~3[c]	200–208	0.223
PS (Dow)	212 000	90 000	8[c]	198–206	0.155
aPA	62 500[b]	29 500[b]	25[d]	220–228	1.000

[a] Typical uncertainty in the molecular weight measurement is 10%
[b] Reported by the supplier
[c] At 200°C
[d] At 265°C

Microscopy

The melt blends were examined using a Jeol 840 scanning electron microscope operated in secondary electron mode. The PS-ox/aPA microstructure was revealed by examining surfaces produced by freezing in liquid nitrogen and subsequent fracturing. In addition, some samples were prepared by etching the fracture surfaces in toluene to remove the PS-ox component, creating higher contrast images which were used for determination of particle size. Images were analysed using commercial software. Average particle size and particle size distributions reported represent the contribution from at least 80 particles measured for each blend.

Fourier transform infra-red (FTi.r.) spectroscopy

Samples for the quantitative *FT*i.r. study were prepared by separating the PS-ox and aPA components from the blends after processing. Warm *N,N*-dimethyl formamide (DMF) was used to dissolve the blended material, and the PS-ox component was then separated from the DMF solution using excess toluene (a non-solvent for aPA), resulting in an aPA precipitate and a solution of PS-ox in toluene/DMF. The aPA precipitate was then removed and the PS-ox was recovered by precipitation into methanol. The solvent separation process was repeated twice on each of the precipitates to ensure separation and then the precipitates were dried at 160°C under vacuum. Dilute blends of PS-ox in aPA and dilute blends of aPA in PS-ox used for calibration were prepared by solution-casting from warm DMF followed by drying under vacuum at 160°C. Films for *FT*i.r. measurements were prepared by pressing a few milligrams of polymer between Teflon-coated aluminium sheets in a Carver press at 180–200°C. Data reported are an average of at least 64 scans.

Fracture toughness

Interfacial adhesion was quantified by measuring interfacial fracture toughness using the asymmetric double cantilever beam test (ADCB)[5]. Toughness is quantified by measurement of the critical energy release rate for interfacial failure (G_c) under constant displacement conditions. The displacement is achieved by inserting a razor blade into the interface of a bilayer constructed from the two immiscible polymers. The bilayer separates ahead of the blade forming an interfacial crack. The crack is grown along the interface by advancing the razor blade at a slow and steady rate (*Figure 2*), and is monitored until a constant length is attained indicating that steady-state conditions have been reached. This steady-state crack length is recorded at fixed intervals during the interfacial failure, and is used in conjunction with material elastic constants to calculate G_c according to the relation:

$$G_c = \frac{3\Delta^2 E_1 h_1^3 E_2 h_2^3}{8a^4} \frac{E_1 h_1^3 C_2^2 + E_2 h_2^3 C_1^2}{(E_1 h_1^3 C_2^2 + E_2 h_2^3 C_1^2)^2} \qquad (1)$$

where a is the crack length, E_i are the Young's moduli of the two polymers, h_i are the thicknesses of the individual polymer layers, Δ is the thickness of the razor blade, and $C_i = 1 + 0.64 h_i/a$ (refs 5, 32). The asymmetry in the testing geometry ($h_1 \neq h_2$) is necessary to compensate for differences in the elastic constants and deformation

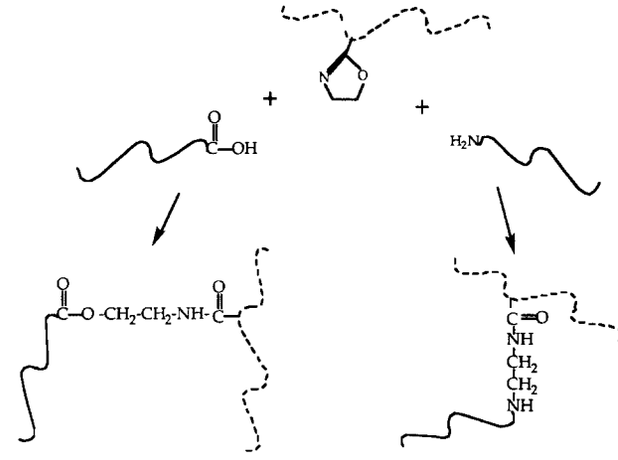

Figure 1 Schematic representation of the grafting reactions between vinyl oxazoline and aPA end-groups: (-) aPA chain; (–) PS chain

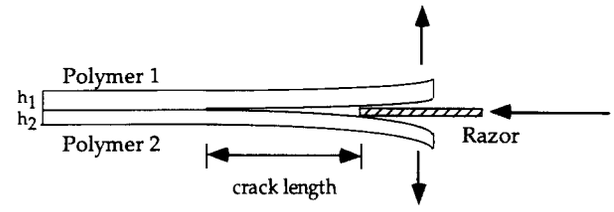

Figure 2 Schematic representation of the ADCB test

characteristics of the two materials on either side of the interface. Additional details about the testing procedure and the ADCB test can be found in refs 5, 8, 33, 34.

Interfacial failure was achieved by inserting a razor blade at the bilayer interface at a constant speed of 3×10^{-6} m s^{-1} using a stepping motor controlled by a programmable microstepping indexer. Crack growth was monitored through the transparent PS beam from above the sample via a video camera. This procedure typically allowed for 20 measurements of crack length per sample. Interfacial fracture toughness, G_c, was calculated according to equation (1) from the measured crack lengths and values of the elastic constants determined by flexure tests which are discussed below. Values of G_c reported are an average of 10–20 measurements per sample in the steady-state regime. All error bars represent plus or minus one standard deviation.

Samples for fracture toughness measurements were prepared by first moulding individual polymers into plates and subsequently joining a PS or PS-ox plate to an aPA plate in a separate step. Individual plates, 1–2.5 mm thick, were prepared by compression-moulding. Typical moulding temperatures for polystyrenes were 150–185°C, and for aPA ~200°C. Bilayers for interfacial fracture testing were made by joining PS and aPA plates under slight contact pressure at 170–185°C for 1 h. After the joining period was complete the pressure was released and the laminates allowed to cool slowly in the moulds over a period of 1–1.5 h to minimize thermal stresses. All plates were dried for at least 16 h at 50–70°C under vacuum immediately prior to the bonding step. After cooling, the edges of the plates were trimmed and the remaining material cut into strips 9–10 mm wide for testing. Some test strips were annealed after joining under flowing nitrogen at 150°C to evaluate effects from the kinetics of the grafting reaction. All PS-ox/aPA

bilayer samples were dried at 80°C under vacuum for at least 12 h immediately prior to testing.

Flexural properties

Mechanical properties were measured for all materials in three-point bending according to the geometry defined in ASTM D790[34] using a Sintech 20 testing machine. Samples for flexural testing were made by compression-moulding as described above. Tests were performed at a crosshead speed corresponding to a strain rate at the outer fibre of the sample of $1.2 \times 10^{-5}\,m\,s^{-1}$, which is a good approximation to the strain rates imposed on the bilayers during interfacial fracture testing[8] of 10^{-5}–$10^{-7}\,m\,s^{-1}$. Modulus values (average ± standard deviation) were found to be: $E_{aPA} = 2.4 \pm 0.11$ GPa; $E_{PS-a} = 3.4 \pm 0.44$ GPa; $E_{PS-ox} = 3.4 \pm 0.20$ GPa.

RESULTS AND DISCUSSION

Morphology studies

Processing pre-tests were performed on the aPA and various polystyrenes prior to blending, in order to choose an unreactive control polystyrene whose rheological properties under the blending conditions match those of the reactive polystyrene as closely as possible. In this way parameters such as the viscosity ratio between the blend components, which is known to influence the dispersed phase size in two-phase blends[32,35], are held constant ensuring that any observed changes between the PS-ox/aPA blends and the PS/aPA blends are a consequence of reactive compatibilization. For the purpose of this investigation the viscosity ratio is represented by a torque ratio obtained by dividing the torque of the various polystyrenes by that of aPA, in all cases measured after 10 min of mixing in the Banbury mixer under identical conditions to those employed for blending[36]. Torque ratios are listed in *Table 1* along with polymer molecular weights and melt indices reported by the suppliers. The PS chosen for blending studies, Dow Styron 666, has rheological properties similar to those of PS-ox, which should allow for direct comparison of the morphology in PS/aPA and PS-ox/aPA blends.

The addition of the oxazoline functionality to the PS molecules causes significant changes in the morphology of PS/aPA blends, as illustrated by the scanning electron micrographs shown in *Figures 3* and *4*. (In *Figure 4* the PS particles have been removed by etching with toluene to show more clearly the location of the particles.) Quantitative image analysis indicates that the average size of the dispersed PS-ox particles in the reactive PS-ox/aPA blend is ~60% smaller than the average size of the dispersed PS particles in the unreactive PS/aPA blend. (Particle size is represented by an equivalent diameter, which is calculated from the measured area of the particle assuming spherical shape). The particle size distributions and their characteristics are illustrated in *Figure 5* and *Table 2*, respectively. Since the blends were processed under identical conditions, and the polystyrenes have very similar melt properties, the observed change in the morphology may be attributed directly to the effects of reactivity. The refinement of the microstructure implies the formation of compatibilizing copolymers which reduce interfacial tension and stabilize the dispersion[32,35,37].

In addition to having a smaller average particle size,

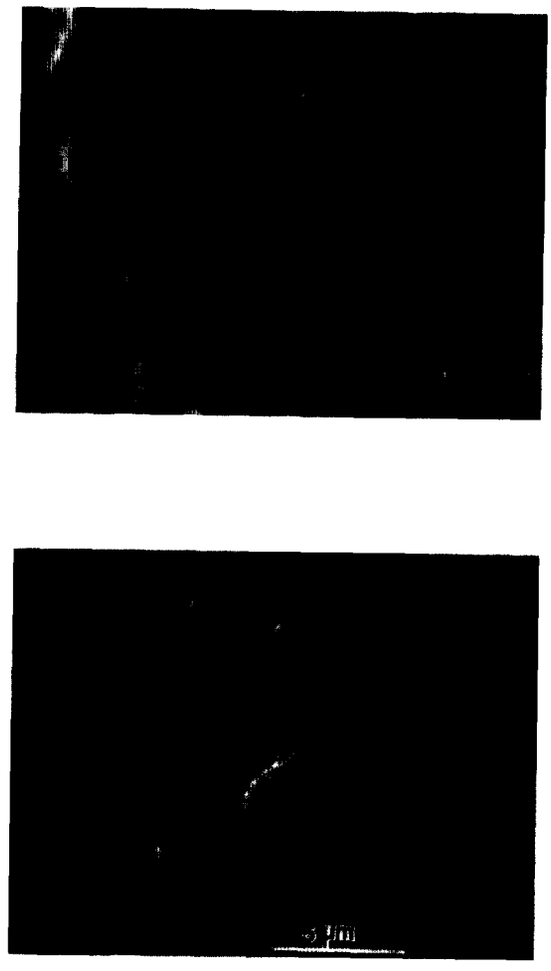

Figure 3 Scanning electron micrographs of 20/80 blends: (a) unreactive PS/aPA blend; (b) reactive PS-ox/aPA blend

the breadth of the particle size distribution in the PS-ox/aPA blend is much smaller than in the PS/aPA blend (*Table 2*, *Figure 5*). This suggests that coalescence effects may be more important in determining the final droplet size in the unreactive system than in the corresponding reactive system, an effect which has been observed previously[38–41]. Further evidence for the importance of coalescence may be gained from comparison of estimated particle size in dilute systems with actual particle size measured. The particle size in the dilute concentration limit may be estimated using the Taylor[38] equation:

$$d = \frac{\gamma_{AB}}{G\eta_m}\frac{16\lambda + 16}{19\lambda + 16}$$

where d is the particle diameter, γ_{AB} is the interfacial tension between blend components A and B, G is the shear rate, and λ is the ratio between the dispersed phase viscosity and the matrix phase viscosity, η_d/η_m. (The Taylor theory of droplet breakup was developed for the case of a Newtonian droplet suspended in a Newtonian fluid under a steady shear flow, and is not strictly applicable to blended polymer systems; however, it provides conceptual understanding and is an accepted starting point for most modern work on droplet dispersion and coalescence[32,35].) For the unreactive blend, the viscosity ratio is approximated by the torque ratio (*Table 1*), the matrix viscosity is ~10 kPa s[42,53], the shear rate is $G \sim 0.75S \sim 37.7\,s^{-1}$ (ref. 36) where $S = 50$ rev

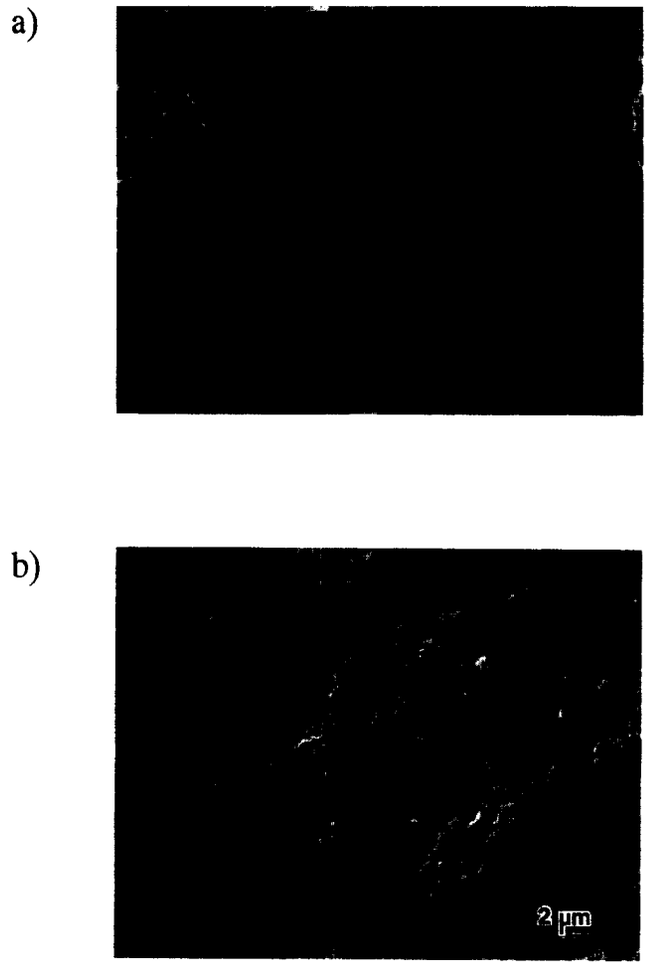

Figure 4 Scanning electron micrographs of 20/80 blends. Samples have been etched to remove the PS particles for enhanced contrast. (a) Unreactive PS/aPA blend; (b) reactive PS-ox/aPA blend

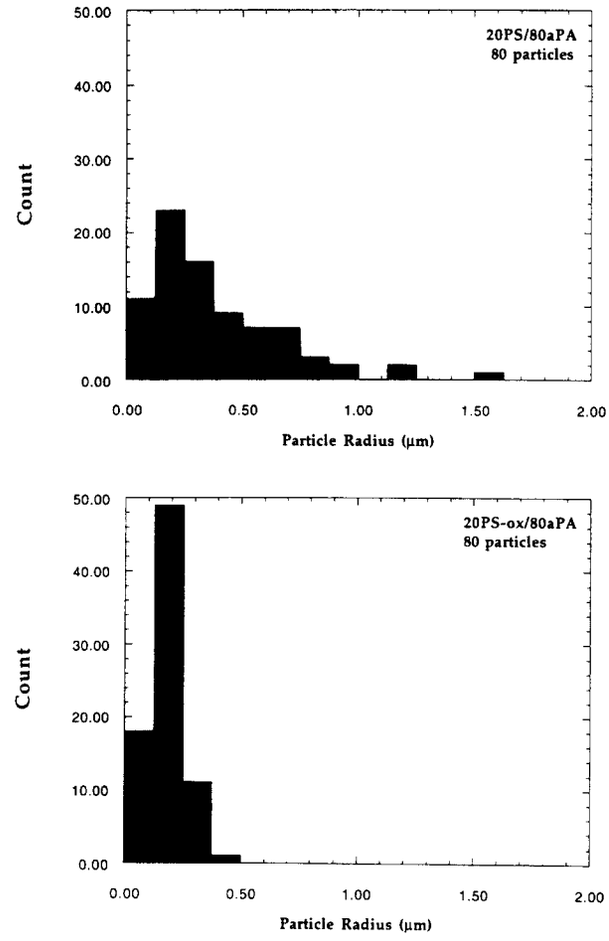

Figure 5 Particle size distributions in PS/aPA melt blends

min^{-1} is the mixing speed, and the interfacial tension is taken as $0.018\,N\,m^{-1}$ from measurements on a similar system[42]. Using these parameters, the Taylor theory predicts $r \sim 0.025\,\mu m$, an order of magnitude smaller than measured, which implies that coalescence effects are important in the 20:80 blends. For this reason, very dilute blends of both types were mixed in a 1:99 ratio with the intention of evaluating particle sizes under conditions which are less sensitive to coalescence. The etched microstructures of the 1:99 blends are shown in *Figure 6*. Due to the very small size of the particles, it was not possible to observe them clearly enough for quantitative analysis. Estimates made from the micrographs indicate that the dispersed phase size in both PS/aPA and PS-ox/aPA blends are in the range of 0.01 to 0.1 μm. A comparison of particle sizes in the dilute 1:99 blends and the 20:80 blends suggests that the particle size is more strongly dependent on concentration in the unreactive blend than in the reactive blends, which again implies a more significant contribution of coalescence in the uncompatibilized system. Similar behaviour has been observed in PS/elastomer blends[38,39] where the average size of the dispersed second phase was found to be insensitive to concentration changes in reactive blends, while increasing with concentration for the unreactive blend counterparts.

The morphology findings from the 20/80 blends

Table 2 Characteristics of the particle size distributions in 20/80 melt blends

Blend identification	Mean particle radius (μm)	Median particle radius (μm)	Standard deviation (μm)	95% confidence interval (μm)
PS-ox/aPA	0.18	0.18	0.07	0.16–0.20
PS/aPA	0.46	0.32	0.78	0.23–0.69

illustrate the magnitude of the compatibilization effect caused by the incorporation of the oxazoline group into polyamide blends; ~1.2 mol% of reactive oxazoline groups, in the presence of reactive aPA end-groups (~1.8 mol%), resulted in the formation of copolymers and a reduction in the average size of dispersed particles of ~60%. Though the observed refinement of the morphology in the PS-ox/aPA blends relative to PS/aPA blends was substantial, the effects were modest in comparison to other investigations of reactive compatibilization. For example, average particle size was reduced by a factor of four in PS/aPA blends in which the PS was functionalized with maleic anhydride[42], and the same reactive chemistry produced a decrease in average particle size of more than an order of magnitude in PS/Nylon 6 blends[43]. The final morphology developed in reactive, immiscible blends is known to be a function of both processing history[21,22] and the level of reactivity

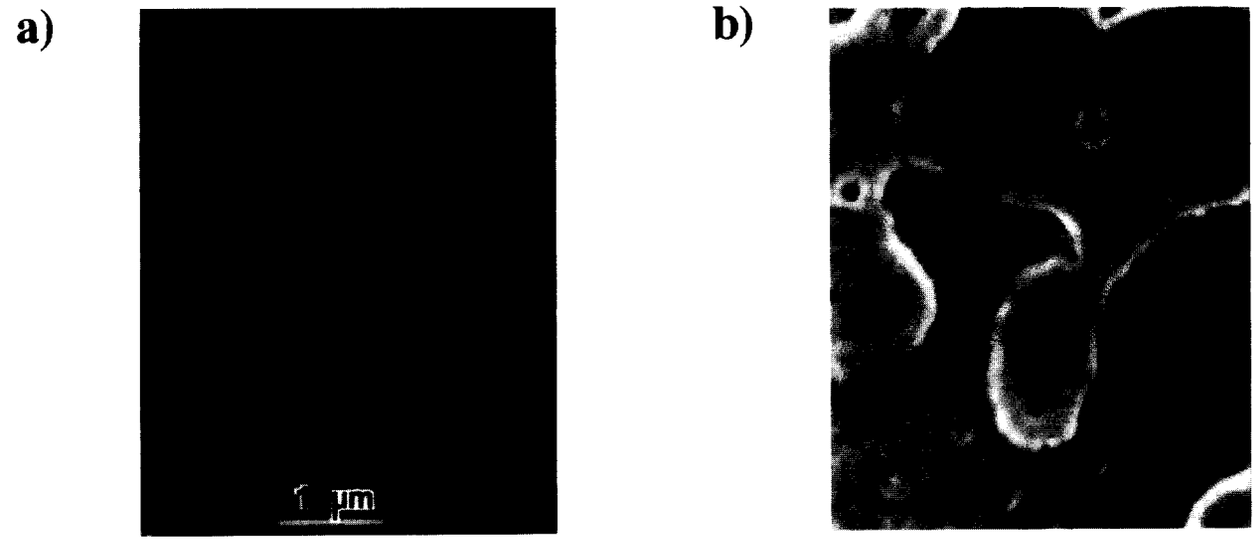

Figure 6 Scanning electron micrographs of 1 : 99 blends. (a) Unreactive 1PS/99aPA blend; (b) reactive 1PS-ox/99aPA blend

in the system[3,18,21,22], thus the apparent disparity between the current results and other studies is believed to be reflecting differences in these factors, particularly the low overall reactivity of the PS-ox/aPA system.

Infra-red spectroscopy

The nature of the compatibilizing reaction was investigated using Fourier transform infra-red (*FT*i.r.) spectroscopy, with the aim of directly confirming the generation of copolymers and quantifying the extent of the grafting reaction. Unfortunately, it was not possible to confirm the reaction mechanisms directly in PS-ox/aPA blends (*Figure 1*) owing to overlap of the absorption bands of the monomers with those of the reactive groups. However, the reactivity of oxazolines with both amines and carboxylic acids has been previously verified[28,44,45].

An extraction technique was employed to prepare samples for *FT*i.r. used to verify and quantify copolymer formation which involves separating the blend into its PS-ox and aPA components by exploiting the difference in solubility characteristics between these two polymers[46]. After the solvent separation the PS-ox and aPA components are each examined using *FT*i.r. for evidence of the characteristic absorption bands of the other component. The unreactive blend is subjected to the identical procedure and similarly evaluated as a control to ensure that the separation process is successful.

*FT*i.r. spectra of PS and PS-ox extracted from the respective 20/80 melt blends are shown in *Figure 7*. The arrow indicates the occurrence of an absorption band at $\sim 3310\,cm^{-1}$ in the spectrum from the extracted PS-ox component which is absent from the pure PS-ox spectrum (*Figure 8*). This absorption is characteristic of N–H stretching in the secondary amide group present along the aPA backbone[47] and is one of the strongest absorptions from pure aPA to occur in a frequency range where PS absorptions are minimal (*Figure 8*). A faint absorption at $\sim 3310\,cm^{-1}$ is present in the PS fraction from the unreactive blend (*Figure 7*), indicating that some aPA remains in the control blends either due to incomplete separation of the components or some small amount of processing-induced grafting unrelated to the oxazoline reaction. The aPA absorption is much stronger

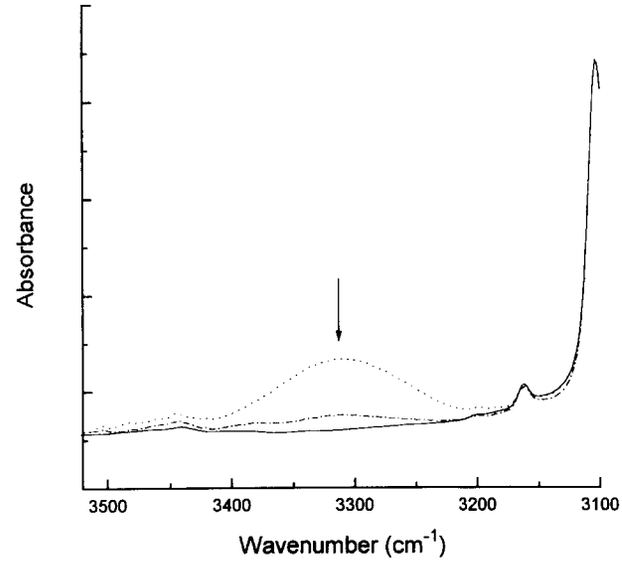

Figure 7 *FT*i.r. spectra of (-) pure PS-ox, and (---) PS and (··) PS-ox extracted from the respective 20/80 blends in aPA. The arrow indicates the peak associated with residual aPA. Spectra have been scaled to account for differences in film thickness

in the spectrum of the PS-ox separated from the reactive blend than in the spectrum of the PS separated from the unreactive blend, providing direct evidence for the *in situ* formation of copolymers in the reactive blend.

The identification of PS residuals in aPA was more difficult than the opposite case, due to the fact that the strongest absorptions from the PS molecule overlap with the characteristic absorptions of aPA (*Figure 8*). The least ambiguous feature which could be attributed to PS in dilute PS/aPA blends was a shoulder occurring on the aPA peak centred at $\sim 925\,cm^{-1}$ (*Figure 9*). Spectra from aPA extracted from the PS/aPA and PS-ox/aPA melt blends showed a slight shoulder in this region, nearly identical in magnitude for both the reactive and unreactive cases, and indicative of a residual PS-ox weight fraction of $\leq 0.5\%$ (*Figure 10*). Because the apparent weight fraction of PS-ox in the aPA fraction from the reactive blend is not significantly different from the

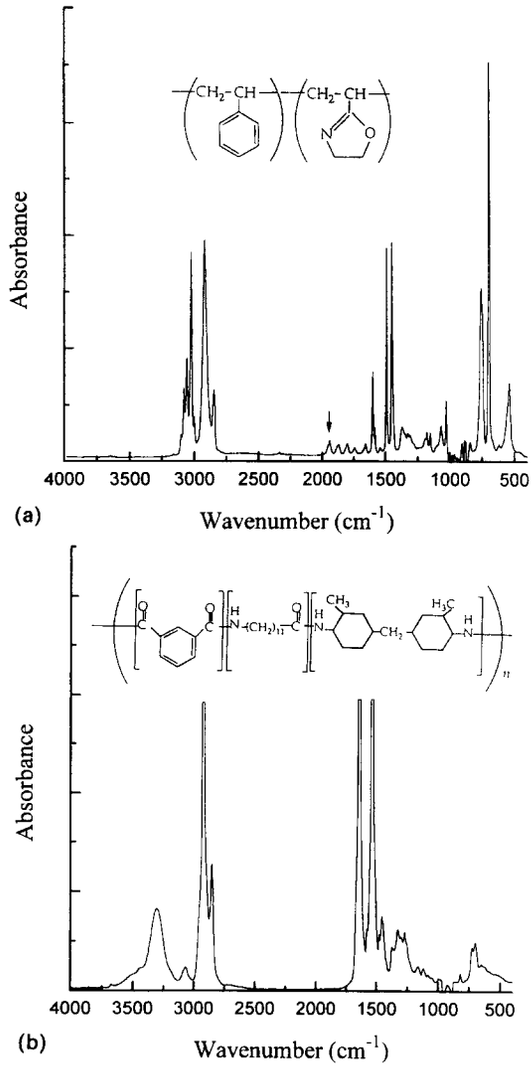

Figure 8 (a) The *FT*i.r. spectrum of pure PS-ox. The arrow indicates the peak used as an internal reference for calibration purposes. (b) The *FT*i.r. spectrum of pure aPA

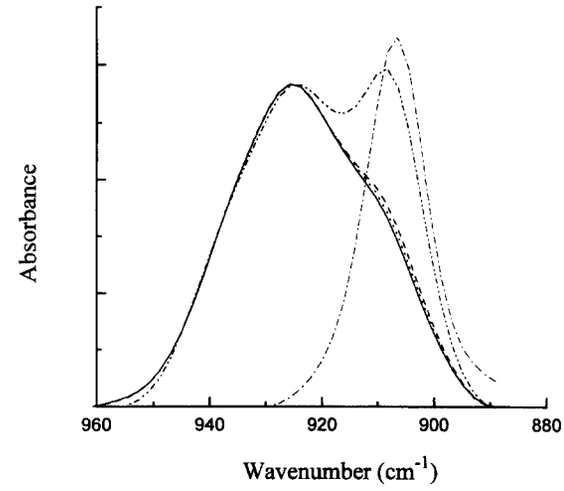

Figure 9 *FT*i.r. spectra for (-) pure aPA, (----) 20% PS in aPA (melt blend), (··) 1.0% PS in aPA, (–) 3.0% PS in aPA, and (---) pure PS. aPA and blend spectra have been scaled to account for differences in film thickness. PS has been scaled arbitrarily

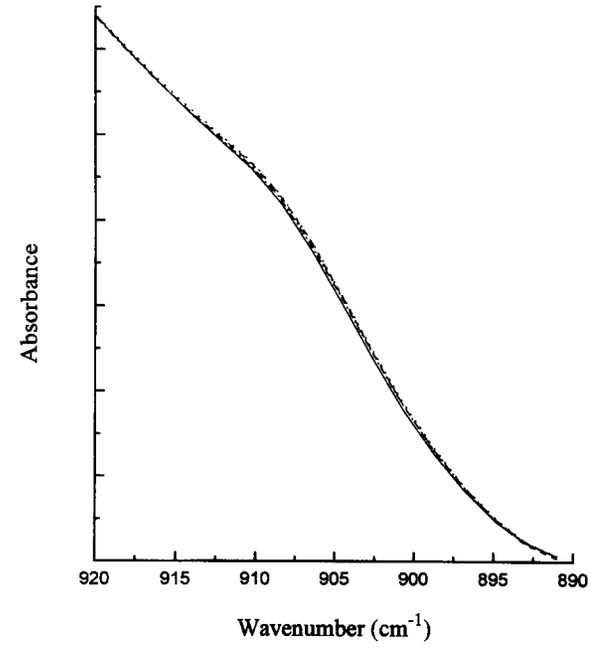

Figure 10 *FT*i.r. spectra from (-) pure aPA, (---) aPA extracted from the unreactive melt blend, (··) aPA extracted from the reactive melt blend, and (–) 0.5% PS in aPA

control, the residual PS-ox observed cannot be unambiguously attributed to copolymers formed by aPA end-group/oxazoline grafting. Therefore, it will be assumed that the concentration of copolymers attributable to oxazoline grafting in the aPA extracted from the reactive blend is negligible.

Quantitative analysis of the spectrum from the PS-ox extracted from 20/80 melt blend was performed to estimate the amount of PS-*g*-aPA copolymer formed during blend processing. The absorbance, A, of a given constituent in a mixture is related to its concentration, c, according to Beer's law:

$$A = \log \frac{I_o}{I} = abc \qquad (2)$$

where b is the thickness of the absorbing medium and a is the absorptivity[48]. This relationship between A and c may be exploited to gain information about the concentration of the mixture if a suitable calibration is available. For the present purposes, a calibration curve has been generated from unreactive aPA/PS solution blends with aPA weight fractions (c_{aPA}) of $\leq 5\%$. The effects of varying film thickness were compensated for by normalizing the aPA absorption at 3310 cm^{-1} (A_{aPA}) relative to a characteristic PS absorption at 1950 cm^{-1} (A_{PS}). The calibration curve was fitted using linear regression, yielding the relation $A_{aPA}/A_{PS} = 0.006 + 0.086c_{aPA}$, with regression coefficient $R^2 = 0.996$. These fitting parameters are subsequently used along with A_{aPA}/A_{PS} measured from the spectra shown in *Figure 6* to calculate the weight fraction of aPA in the PS and PS-ox components extracted from the respective melt blends. The results are $c_{aPA} = 0.3\%$ in the PS from the unreactive 20/80 PS/aPA blend, and $c_{aPA} = 3.3\%$ in the PS-ox from the reactive 20/80 PS-ox/aPA blend. It was assumed that the residual aPA that was observed in the extracted PS and is not attributable to oxazoline grafting is also present in the extracted PS-ox, therefore the weight fraction of aPA in the PS-ox due to PS-ox-*g*-aPA

copolymers is corrected to $c_{aPA}^{copolymers} = 3.3 - 0.3 = 3.0\%$. This concentration may be readily converted into total copolymer concentration in the blend using the polymer molecular weights listed in *Table 1* and the assumption of one PS-ox/aPA bond per copolymer chain, yielding a total compatibilizer concentration of ~2.5% (see Appendix 1). This concentration may be considered a lower bound, due to possible loss of some copolymers during the solvent separation process.

A calculation similar to the one described above shows that only ~10% of all PS chains and ~0.8% of all aPA chains are grafted (Appendix 1). This result brings up an interesting point concerning the concentration of reactive groups necessary for compatibilization in the PS-ox/aPA system. With ~10% of PS-ox chains grafted and $N_{ox} \approx (0.0118)M_n^{PSox}/M^{styrene} \approx 10$ reactive monomers per chain, less than 1% of all of the available oxazoline groups participated in a grafting reaction under the current processing conditions. A similar consideration implies that <0.5% of all aPA end-groups participate in a grafting reaction. These results suggest that a large excess of functional groups is necessary to promote compatibilization in PS-ox/aPA blends, and may be indicative of low reactivity between oxazoline and polyamide end-groups.

Interfacial adhesion between PS-ox and aPA

The effects of reactivity on the adhesion between PS and aPA was evaluated using the asymmetric double cantilever beam test which isolates the interfacial properties by using a model testing geometry. The interfacial fracture toughness was measured as a function of the thickness ratio of each component, $h_{PS}/(h_{PS} + h_{aPA})$, to determine the sensitivity of the measurement to the difference in elastic constants between the components. (Measurements performed using improper geometry have been previously shown to yield erroneous results[5,8,33].) In the PS-ox/aPA system, interfacial fracture toughness is insensitive to asymmetry ratio over the range 0.3–0.6, and no wandering of the crack path away from the interface was observed. These conditions indicate that failure is occurring along the interface and ensure that adhesive rather than cohesive properties are being measured.

The effects of asymmetry ratio and reactivity on the interfacial fracture toughness of PS/aPA bilayers are illustrated in *Figure 11*. Although there is some scatter in the data, one may state with at least 99.5% confidence that the average fracture toughness of the reactive interface is greater than that of the unreactive interface. Analysis of all data points shown yields: $\langle G_c \rangle_{reactive} = 10.2\,J\,m^{-2}$, where $7.6 < \langle G_c \rangle_{reactive} < 12.8\,J\,m^{-2}$ represents a 95% confidence interval for the PS-ox/aPA interface, and $\langle G_c \rangle_{unreactive} = 3.8\,J\,m^{-2}$ where $1.8 < \langle G_c \rangle_{unreactive} < 5.8\,J\,m^{-2}$ represents a 95% confidence interval for the PS/aPA interface. Thus the toughness of the reactive interface is significantly increased relative to the unreactive interface with an improvement in the average toughness of ~170%.

An attempt was made at further improving the interfacial grafting density and consequently the interfacial toughness through extension of the reaction time over a period of several days. In this experiment, several strips were cut from the same sample plate, which was joined at 185°C for 1 h, and were heat-treated for periods of up to 100 h under nitrogen before interfacial fracture testing. The heat treatment temperature was set at 150°C, just below the T_g of aPA, to ensure that the samples maintained geometrical integrity if supported by the aPA beam, but far enough above the T_g of PS-ox to allow for some molecular rearrangement. The results are shown in *Figure 12*. G_c increases approximately linearly from ~ 8 to ~ 13 J m^{-2} as the time held at temperature increases. Apparently, the low reactivity in this system prohibits the generation of a high enough grafting density to achieve large increases in interfacial toughness.

Although the reactive interface does exhibit superior toughness relative to its unreactive counterpart, the magnitude of the effect is small when compared with the results of previous studies[5–8,24,25,49,50]. These studies have shown that low toughness is observed under conditions where the copolymer blocks are shorter than the entanglement molecular weight, or when the grafting density at the surface is low[6–8,49,50]. The PS segments of the copolymer chains should be considerably longer than the entanglement molecular weight[8] of ~27 000 g mol^{-1}. The entanglement molecular weight of the aPA material

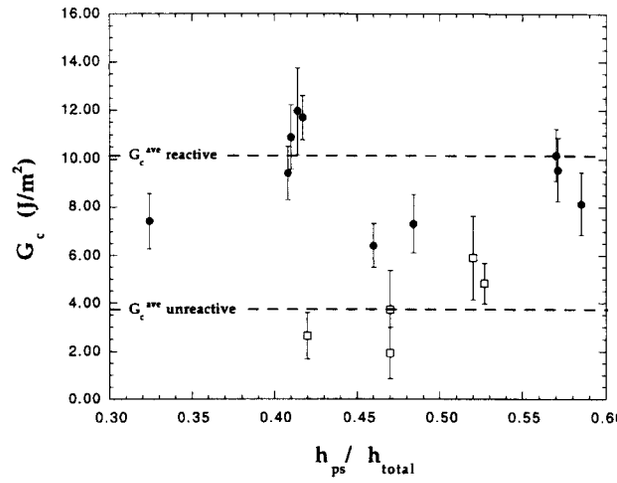

Figure 11 The critical energy release rate for interfacial fracture *versus* ratio of PS beam thickness to total bilayer thickness (beam joining conditions, 175 ± 10°C/1 h). ●, PS-ox/aPA; □, PS/aPA

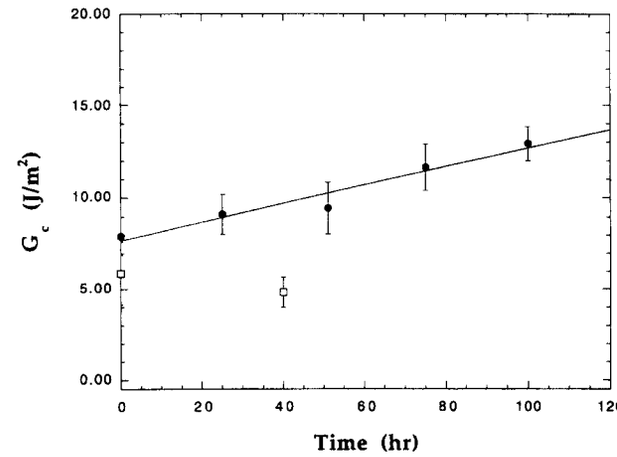

Figure 12 The critical energy release rate for interfacial fracture *versus* reaction time at 150°C. ●, PS-ox/aPA; □, PS/aPA

is not known, but since entanglement typically occurs at ~400 backbone chain atoms or less[51], and the estimated number of backbone chain atoms for aPA is greater than 3000, it is fair to assume that the average length of both segments of the copolymer is sufficiently long to provide entanglement. Thus the observed interfacial toughness most likely reflects a low grafting density at the PS-ox/aPA interface resulting from low levels of reactivity in this system. It was not possible to measure the grafting density at the idealized PS-ox/aPA interface used in the fracture toughness experiments; however, an approximation of the interfacial areal density of copolymers (Σ) may be made by assuming that the percentage of the PS-ox beam surface which is reactive is equal to the percentage of reactive monomer sites on the surface. The calculation, detailed in Appendix 2, cannot account for surface segregation/desegregation of oxazoline, diffusion effects or reaction kinetics, but gives a first approximation to the grafting density of $\Sigma \sim 0.03$ reactive sites nm^{-2}. Previous experiments on block copolymer reinforced interfaces typically associate fracture toughness of $\sim 10\,J\,m^{-2}$ with an interfacial copolymer junction density of[7,8] $\Sigma \sim 0.01$–0.04 bonds nm^{-2}, in reasonable agreement with the current results.

One aim of this study was to gain some insight into the interfacial properties of blends processed under practical conditions. However, the area density of copolymer joints at the PS-ox/aPA interface of the bimaterial beams used for the fracture test may not necessarily be a good approximation to the joint density across the particle interfaces in the melt blend due to differences in the sample preparation. A better understanding of the effects of graft copolymer formation on the interfacial adhesive properties in the PS-ox/aPA blends may be gained from evaluating the interfacial areal density of grafts produced during the processing. The graft density at the interphase interfaces in the melt blend may be estimated using the quantitative information obtained in the *FT*i.r. experiments in combination with an average interfacial area per unit volume determined from the particle size measurements. The calculation, detailed in Appendix 1, yields an estimated interfacial graft density of $\Sigma \sim 0.04$ chains nm^{-2}. Based on this estimate for Σ, the current findings, and the results of previous studies[7,8], the expected change in the adhesion at the PS-ox/aPA interfaces in the melt blend due to the incorporation of 1.2 wt% of oxazoline would be an improvement of 100% or more.

SUMMARY

The reactive compatibilization of a PS/aPA blend by functionalization of PS with oxazoline groups has been described. Incorporation of 1.2% vinyl oxazoline into PS chains facilitated the *in situ* formation of PS-*g*-aPA copolymers by grafting between oxazoline and aPA endgroups resulting in desirable modifications to blend properties. The morphology of the blend was modestly refined due to copolymer formation, with the dispersed phase size in the reactive, 20/80 PS-ox/aPA blend reduced ~60% relative to the comparable unreactive blend. A quantitative evaluation of the compatibilizing reaction indicated that the reactive blend contained ~2.5% of PS-*g*-aPA copolymer which formed during processing through the reaction of <1% of oxazoline groups present, resulting in aPA grafts on ~10% of PS-ox chains. In addition to morphology refinement, the *in situ* grafting reaction was shown to provide some mechanical reinforcement of PS/aPA interfaces. The adhesion at the reactive PS-ox/aPA interface was found to be improved at least two-fold relative to the comparable unreactive PS/aPA interface.

ACKNOWLEDGEMENTS

The assistance of Dr Joy Dunkers of the National Institute of Standards and Technology with *FT*i.r. is gratefully acknowledged. Financial support for N.C.B.T. was provided by the NDSEG Fellowship Program.

REFERENCES

1 Paul, D. R. and Newman, S. (Eds) 'Polymer Blends', Academic Press, New York, 1978, Vol. 2
2 Rudin, A. *Makromol. Sci. Rev. Macromol. Chem.* 1980, **C19**, 267
3 Paul, D. R. and Barlow, J. W. 'Encyclopedia of Polymer Science and Engineering', 2nd Edn, John Wiley & Sons, New York, 1986, p. 399
4 Liebler, L. *Makromol. Chem., Macromol. Symp.* 1988, **16**, 1
5 Brown, H. R. *J. Mater. Sci.* 1990, **25**, 2791
6 Washiyama, J. *et al. Macromolecules* 1994, **27**, 2019
7 Creton, C., Brown, H. R. and Deline, V. R. *Macromolecules* 1994, **27**, 1774
8 Creton, C. *et al. Macromolecules* 1992, **25**, 3075
9 Creton, C., Kramer, E. J. and Hadziioannou, G. *Macromolecules* 1991, **24**, 1846
10 Washiyama, J., Creton, C. and Kramer, E. J. *Macromolecules* 1992, **25**, 4751
11 Reichert, W. F. and Brown, H. R. *Polymer* 1993, **34**, 2289
12 Brown, H. R. *Macromolecules* 1993, **26**, 1666
13 Brown, S. B. 'Reactive Extrusion, Principles and Practice' (Ed. M. Xanthos), Hanser Publishers, New York, 1992, p. 75
14 Liu, N. C. and Baker, W. E. *Adv. Polym. Tech.* 1992, **11**, 249
15 Xanthos, M. and Dagli, S. S. *Polym. Eng. Sci.* 1991, **31**, 929
16 Liu, N. C., Baker, W. E. and Russell, K. E. *J. Appl. Polym. Sci.* 1990, **41**, 2285
17 Angola, J. C. *et al. J. Polym. Sci., Polym. Phys.* 1988, **26**, 807
18 Fowler, M. W. and Baker, W. E. *Polym. Eng. Sci.* 1988, **28**, 1427
19 MacKnight, W. J. *et al. Polym. Eng. Sci.* 1985, **25**, 1124
20 Song, Z. and Baker, W. E. *J. Appl. Polym. Sci.* 1992, **44**, 2167
21 Liu, N. C. and Baker, W. E. *Polymer* 1994, **35**, 988
22 Liu, N. C. and Baker, W. E. *Polym. Eng. Sci.* 1992, **32**, 1695
23 Liu, N. C. and Baker, W. E. *PMSE Preprints* 1992, **67**, 305
24 Lee, Y. and Char, K. *Macromolecules* 1994, **27**, 2603
25 Beck Tan, N. C., Peiffer, D. G. and Briber, R. M. *Macromolecules* in press
26 Saleem, M. and Baker, W. E. *J. Appl. Polym. Sci.* 1990, **39**, 655
27 Baker, W. E. and Saleem, M. *Polym. Eng. Sci.* 1987, **27**, 1634
28 Baker, W. E. and Saleem, M. *Polymer* 1987, **28**, 2057
29 Fowler, M. W. and Baker, W. E. *Polym. Eng. Sci.* 1988, **28**, 1427
30 Ellis, T. S. *Macromolecules* 1991, **24**, 3845
31 Freakly, P. K. and Wan Idris, W. Y. *Rubber. Chem. Tech.* 1979, **52**, 134
32 Wu, S. *Polym. Eng. Sci.* 1987, **27**, 335
33 Beck Tan, N. C. PhD Dissertation, University of Maryland, 1994
34 Xiao, F., Hui, C.-Y. and Kramer, E. J. *J. Mater. Sci.* 1993, **28**, 5620
35 Utracki, L. A. and Shi, Z. H. *Polym. Eng. Sci.* 1992, **32**, 1824
36 Goodrich, J. E. and Porter, R. S. *Polym Eng. Sci.* 1967, **7**, 45
37 Liebler, L. *Makromol. Chem., Macromol. Symp.* 1988, **16**, 1
38 Taylor, G. I. *Proc. Roy. Soc. London* 1934, **A146**, 501
39 Sundararaj, U. and Macosko, C. W. *Polym. Prepr. Jpn. (Engl. Edn)* 1993, **41**, E-753
40 Willis, J. M., Favis, B. D. and Lunt, J. *Polym. Eng. Sci.* 1990, **30**, 1073
41 Favis, B. D. and Willis, J. M. *J. Polym. Sci., Polym. Phys.* 1990, **28**, 2259
42 Sundararaj, U. *et al. Polym. Eng. Sci.* in press

43 Chen, C. C. *et al. Polym. Eng. Sci.* 1988, **28**, 69
44 Frump, J. A. *Chem. Rev.* 1971, **71**, 483
45 Nishikubo, T., Iiawa, T. and Tokairin, A. *Makromol. Chem., Rapid Commun.* 1981, **2**, 91
46 Briber, R. M. and Bauer, B. J. *Macromolecules* 1988, **21**, 3296
47 Conley, R. T. 'Infrared Spectroscopy', Allyn and Bacon, Inc., Boston, 1966
48 Konig, J. L. 'Spectroscopy of Polymers', American Chemical Society, Washington, DC, 1992
49 Char, K., Brown, H. R. and Deline, V. R. *Macromolecules* 1993, **26**, 4164
50 Brown, H. R. *et al. Macromolecules* 1993, **26**, 4155
51 Ferry, J. D. 'Viscoelastic Properties of Polymers', John Wiley & Sons, New York, 1980
52 Yukioka, S. and Inoue, T. *Polymer* 1994, **35**, 1182
53 'Grilamid TR55 Transparent Nylons', Material Data Sheet supplied by EMS-American Grilon, Inc., Sumter, SC 29151-1717

APPENDIX 1

Calculation of the copolymer concentration in the blend

If c_j^i is the concentration (weight percent) of species j in component i, m_i is the weight of component i, n_i is the number of moles of component i, and MW_i is the molecular weight of polymer i, one may deduce:

$$c_{aPA}^{copolymer}|_{extract} = \frac{m_{aPA}}{m_{aPA} + m_{PS}} = 0.03$$

from which

$$\left.\frac{m_{aPA}}{m_{PS}}\right|_{extract} = 0.03$$

and

$$c_{aPA}^{copolymer}|_{blend} = \frac{m_{aPA}}{m_{PS}}\frac{m_{PS}}{m_{blend}} = 0.03 \times 0.2 = 6.2 \times 10^{-3}$$

yielding

$$\frac{n_{copolymers}}{m_{blend}} = c_{aPA}^{copolymer}|_{blend} \div M_n^{aPA}$$
$$= 6.2 \times 10^{-3}/29\,500 = 2.1 \times 10^{-7}$$

and finally

$$c_{blend}^{copolymer} = \frac{n_{copolymers}}{m_{blend}} * (M_n^{PS} + M_n^{aPA})$$
$$= (2.13 \times 10^{-7})(90\,200 + 29\,500) = 0.025$$

or 2.5% copolymers in the blend, by weight.

Similarly

$$\frac{n_{PS}^{copolymer}}{n_{PS}^{blend}} = \frac{n_{copolymers}}{m_{blend}}\frac{m_{blend}}{m_{PS}}M_n^{PS}$$
$$= (2.1 \times 10^{-7})(1/0.2)90\,200 = 0.095$$

or 9.5% of all PS chains which have a graft, and

$$\frac{n_{aPA}^{copolymer}}{n_{aPA}^{blend}} = \frac{n_{copolymers}}{m_{blend}}\frac{m_{blend}}{m_{aPA}}M_n^{aPA}$$
$$= (2.1 \times 10^{-7})(1/0.8)29\,500 = 0.008$$

or 0.8% of all aPA chains which have a graft.

Estimation of the interfacial areal density of copolymer grafts in the reactive melt blend

The areal density of copolymer joints across the PS-ox/aPA interface may be calculated by using the results of the image analysis of the morphology to estimate the surface area (S) to volume (V) ratio of the blend. From the mean particle size (*Table 2*):

$$\frac{S_{particle}}{V_{particle}} = \frac{4\pi r^2}{\frac{4}{3}\pi r^3} = \frac{3}{r} = 16.7\,\mu m^2/\mu m^3$$

and

$$\frac{S_{particle}}{V_{blend}} = \frac{S_{particle}}{V_{particle}}\frac{V_{particle}}{V_{blend}} = \frac{S_{particle}}{V_{particle}}\frac{m_{PS}/\rho_{PS}}{m_{blend}/\rho_{blend}}$$
$$= 16.7\frac{0.2/1.04}{1.0/(0.2 \times 1.04 + 0.8 \times 1.06)}$$
$$= 3.39\,\mu m^2/\mu m^3$$

where $\rho_{PS} = 1.04$ and $\rho_{aPA} = 1.06$ are the polymer densities ($g\,cm^{-3}$).

From above:

$$\frac{\#\,copolymers}{V_{blend}} = \frac{n_{copolymers}}{m_{blend}}\frac{\#copolymers}{mole}\frac{m_{blend}}{V_{blend}}$$
$$= (2.1 \times 10^{-7})(6.023 \times 10^{23})1.056$$
$$= 1.36 \times 10^{17}$$

and finally

$$\sum = \frac{\#bonds}{S_{particle}} = \frac{\#copolymers}{V_{blend}}\frac{V_{blend}}{S_{particle}}$$
$$= [(1.36 \times 10^{17})/3.39] \times 10^{-18}$$
$$\Sigma = 0.04\ bonds\,nm^{-2}$$

APPENDIX 2

Estimation of Σ at the bimaterial beam interface

The areal density of reactive sites may be estimated in the following manner.

For polystyrene:

$$\rho_{PS} = 1.04\,g\,cm^{-3} = 1.04 \times 10^{-21}\,g\,nm^{-3}$$

and the monomer molecular weight is $M_{mon} = 104\,g\,mol^{-1}$, yielding:

$$\rho_{mon} = 1.04 \times 10^{-21}\,g\,nm^{-3} \times \frac{1\,mol}{104\,g}$$
$$\times 6.02 \times 10^{23} monomers\,mol^{-1}$$
$$= 6.02\,monomers\,nm^{-3}$$

from which

$$V_{mon} = 1/\rho_{mon} = 0.17\,nm^3\ monomer^{-1}$$

and

$$A_{mon} = \pi\left(\frac{3}{4\pi}V\right)^{\frac{2}{3}} = 0.37\,nm^2\ monomer^{-1}$$

or

$$\rho^{A}_{mon} = 2.7 \text{ monomers nm}^{-2}$$

where ρ^{A}_{mon} approximates the surface area per monomer.

Assuming (1) the surface area of an oxazoline monomer is approximately equal to the surface area of a polystyrene monomer, and (2) the areal density of reactive sites is equal to the percentage of reactive surface area yields:

$$\sum = [c_{ox}]\rho^{A}_{mon}$$

or $\Sigma \sim 0.03$ reactive sites nm^{-2}